EAC OF AUSTENITE IN HOT WATER CREVICES MEASURED BY RISING DISPLACEMENT TEST METHOD

Anna Brožová, Karel Šplíchal*

The 08Ch18N10T austenitic steel applied to components in nuclear industry is resistant to environmental assisted cracking in the bulk secondary water. It only suffers from EAC in crevices where SO_4^{2-}, Ca^{2+}, Na^+, SiO_2 and Cl^- are present as main constituents of the concentrated coolant. RDT tests using 0.5T CT specimens were carried out at 270°C in three environments simulating crevices with different concentrations. Values of the threshold K_{ISCC} and the EAC crack growth rate were established for the corrosion systems. The observed crack growth mechanism was transgranular cleavage.

INTRODUCTION

Corrosion damage of WWER 440 steam generators takes place in the secondary circuit under crevice corrosion conditions. In most cases the environmentally affected cracking (EAC) is initiated on the tube outer surface under tube support plates and in thread holes of the primary collector flanges. The prevention of corrosion damage of the primary collectors and tubing is aimed to eliminate the possibility of unstable crack propagation and release of radioactivity. An excessive damage of thread holes necessitates replacing the upper part of a primary collector, in the case of tubes their plugging is required.

Corrosion damage of this type of steel is influenced by aggressive impurities as well as „non-aggressive“ compounds. Sulphates and chlorides as aggressive species and silicates and alumino-silicates as „non-aggressive“ species are present in the crevice environment in significant amounts. Local water chemistry parameters were evaluated using the MULTEQ Code. As input data the measured operational values of local and bulk environments have been used.

MATERIAL AND EXPERIMENT

The experiments were carried out on the 08Ch18N10T (A321) forged austenitic steel of the primary collector. The chemical composition of the steel is shown in Tab.1, the mechanical properties are in Tab.2. The steel microstructure was austenite with equiaxed grains, 50 μm in size, containing many twins and δ-ferrite. For the experiments 12.5 mm thick CT specimens were employed. The specimens were prepared with fatigue pre-cracks and sidegrooves deep 10 % of the specimen thickness.

* Nuclear Research Institute Řež, plc. 25068 Řež, The Czech Republic.

TABLE1- The chemical composition of the steel 08Ch18N10T in wt %.

C	Mn	Si	Cr	Ni	S	P	Ti	N	Cu	Co
0.06	1.33	0.58	18.31	10.8	0.013	0.012	0.55	0.01	0.07	0.03

TABLE2- The mechanical properties of the steel 08Ch18N10T.

Temperature [°C]	σ_Y [MPA]	σ_u [MPA]	A [%]	R.A. [%]
25	261	548	53	63
320	182	392	38	62

The rising displacement test method (RDT) (1,2) is newly developed accelerated SCC test. It is based on the single specimen J-integral test. The crack length was measured during the tests by reversed dc potential drop method. Tests were carried out in a titanium autoclave of 0.5l volume. The chosen temperature was 270°C.

Characterization of the water environment was based on chemical parameters of the blowdown water, on the composition of hideout return at the temperature, when flooding of steam generators takes place, and on analysis of water samples taken from thread holes after opening of the hot collector head analysis (3). For the tests three model environments simulating crevices in steam generator under secondary side water condition were used. The Env I corresponds to the content of species in the thread hole water. Env II and III were established on the base of the blowdown water composition and MULTEQ code concentration factors. Parameters of the environments are specified in Tab.3.

TABLE3- The composition of the test environments, blowdown (BD), thread hole (TH) and MULTEQ code calculated waters (CF is the concentration factor).

	BD	TH	TEST ENVIRONMENT		
[mg/kg]			Env I (CF 10^2)	Env II (CF $4.9*10^4$)	Env III (CF $8.7*10^5$)
Cl	0.016	5.1	5	779	13 856
Na	0.073	9.9	10	3550	63 218
SO_4	0.015	16.1	15	730	12 990
SiO_2	0.057	0.60	300	2260	45 898
Ca	0.102	3.2	40	4970	34 640
Al	0.005	0.053	40	234	4 330
pH_T	-	-	8.2	9.7	10.4

TEST RESULTS

RDT results showed that an environmentally affected cracking (EAC) occurred in testes carried out with the displacement rates ranging from 50 to 5 μm/h in the load line (Fig.1). The effects were observed only in those cases, where the specimens were covered with a deposit layer due to pre-exposition. With decreasing displacement rate decreasing values of K_{ini}, J_{ini} or $J_{0.2}$ were obtained, Fig. 2. Minimum initiation values K_{ini} (K_{ISCC}) or J_{ini} were dependant on the environment. The displacement rate of the minimum was about 7 μm/h in Env I, in Env II and Env III it was 50 μm/h. The lowest K_{ISCC} value was found in Env I; in both more concentrated environments these values were similar.

The J-R curves for all the environments are shown in Fig.3. As can be seen that the slope of the curves decreases with decreasing displacement rate. It even increases due to the influence of the stroke control. The heaviest environmental effect can be observed in Env I.

Assuming that mechanical and environmental effects are additive components of the crack growth rate (4), it is possible to separate the mechanical component from the environmental one. Resulting plots of the environmental crack growth rates vs. J-integral are displayed in Fig. 4. As can be seen, the plateau rate, da/dt_{EAC} , has the value $1.5*10^{-9}$ m/s and it does not changed in any environment.

The fracture surface exhibits the transgranular cleavage fracture mode. The crack growth was initiated in the environments practically without any observable stretch zone (Fig.5). The fact agrees well with measurements of the low initiation fracture toughness values. The sizes of cleavage facets of the surface can be related to the grain size. The cleavage fracture reinitiates on the grain boundaries. The facets are covered with parallel step lines which can be identified as arrest lines (Fig.6). Details of the steps of specimens tested in Env II are shown in Fig.7, 8. In Env III, the environmental crack increments were found both in the pre-crack tip (Fig.9, 10) and in sidegrooves.

DISCUSSION

The EAC fractures were observed to initiate from fatigue pre-cracks covered by deposit layer indicating that the fracture can be promoted by adsorption and chemisorption. According to the adsorption-induced localised-slip model (5) adsorption of atoms weakens interatomic bonds and thereby facilitates the injection of dislocations from the crack tip, bringing about crack growth by an alternate-slip process. The crack grows by ductile mechanisms, which produces small, shallow dimples on the scale of microns. The model is applicable to cleavage-like cracking of many corrosion systems including Fe. The enhanced plasticity model (6) has suggested that localised dissolution along crystallographic planes at crack tips in conjunction with adsorption and chemisorption promotes localised slip along the slip planes. In this case the increments are of the cleavage nature. From the micrographs of specimens (Fig.5-10) cannot be distinguish if fracture is locally cleavage or ductile.

In the maximum concentration environment (Env III) the EAC was initiated also from notches on specimen sides where the constraint is lower than in specimen centre. It was calculated that the constraint value decreases K_{ISCC} (7). Previously it was observed (8) in particular corrosion system that using sidegroove the EAC is primarily initiated from it. This was explained by higher strain rate in sidegrooves than in specimen centre and quicker attainment of the equivalent stress answering to the yield stress. The effect can be concomitant to a dislocation activity based EAC process.

CONCLUSIONS

The 08Ch18N10T steel is sensitive to EAC in concentrated crevice environments based on the presence of sulphates, chlorides, sodium and other aggressive agents. Other species as SiO_2, Ca, Mg and Al can affect the attainment of the resulting pH and porosity as well as sorption properties of the oxide film.

K_{ISCC} values are dependent on the concentration factor; the EAC plateau rates are equal in all environments.

REFERENCES

(1) Dietzel W., K-H. Schwalbe, ECF 10, ESIS, Berlin, 1994.

(2) Dietzel W., CDI'96, Nice, 1996.

(3) Šplíchal K., EPRI Studge Management Workshop, Myrth Beach, 1996.

(4) Karlajajnen-Roikonen P., Wallin K., ECF 9, ESIS, Varna, 1992.

(5) Lynch S.P., CDI'96, EFC 21, ed. T.Magnin, The Institute of Materials, 1997, p.206.

(6) Magnin T.: "Advances in Corrosion-Deformation Interactions", Trans Tech Publications, Zurich, Switzerland (1996).

(7) Suzuki S., Shoji T., 8.International Symposium on Environmental Degradation of Materials in Nuclear Power Systems – Water Reactors, Florida, 1997.

(8) Brožová A., Lauerová D., Ruščák M., CDI'96, Nice, 1996.

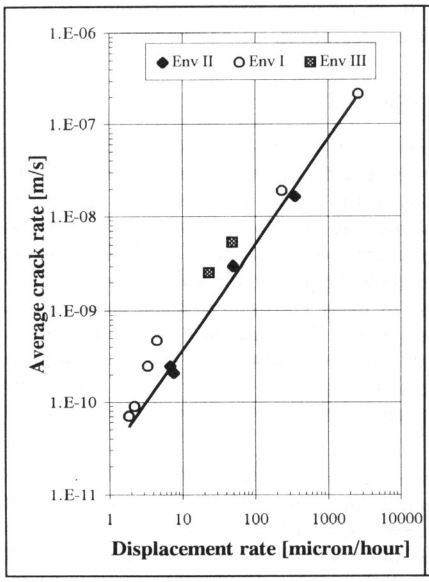

Fig.1: Relation between the average crack velocities and displacement rates.

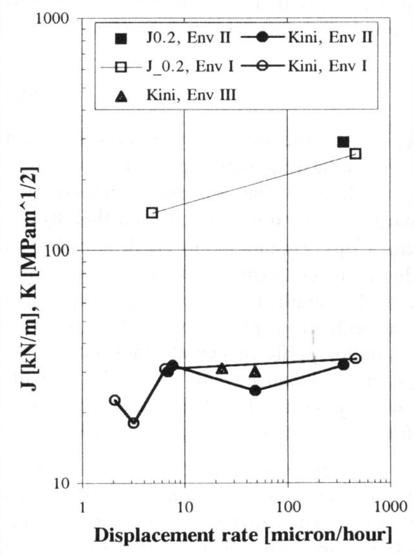

Fig.2: Initiation values of stress intensity factor and J-integral vs. displacement rates.

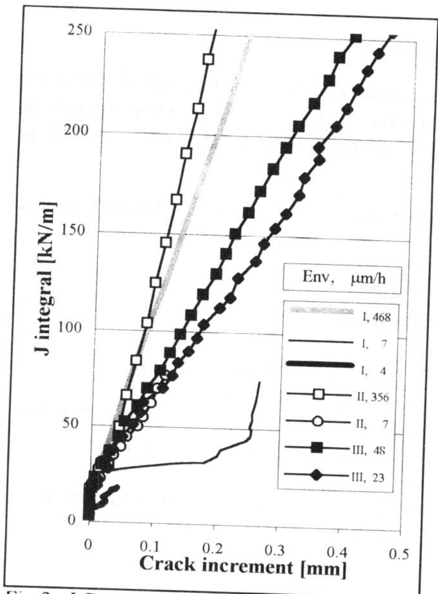

Fig.3: J-R curves of different displacement rates in the three crevice environment.

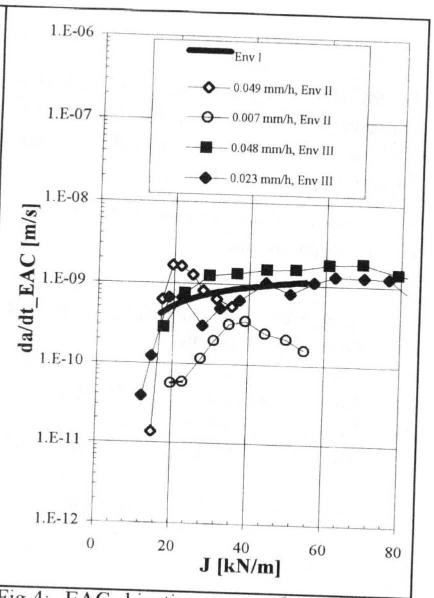

Fig.4: EAC kinetic curves for the three crevice environments.

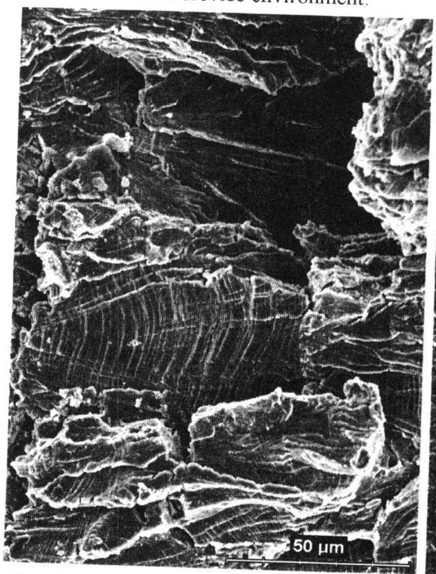

Fig.5: Fracture surface appearance in EnvI, 7 µm/h (crack grows from left to right).

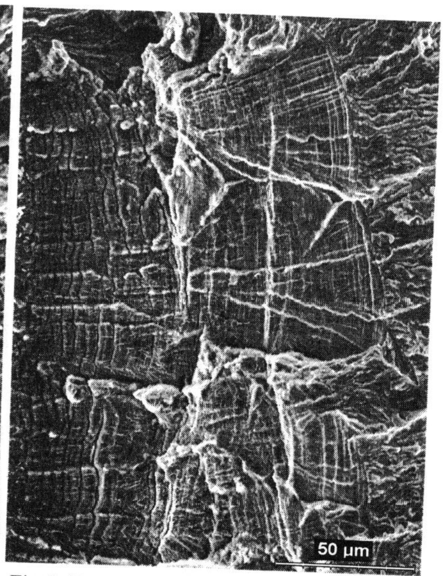

Fig.6: Fracture surface appearance in EnvII, 7 µm/h (crack grows from left to right).

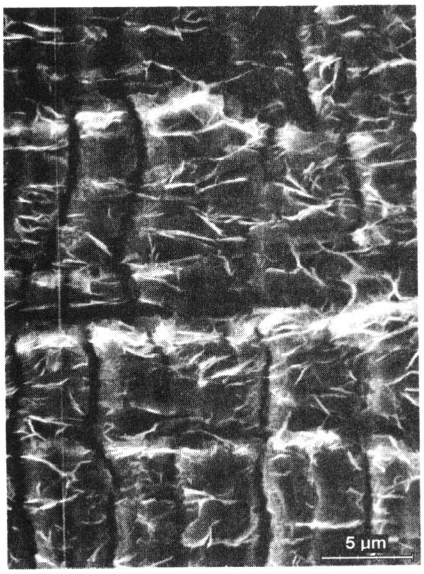

Fig.7: Detail of the surface in EnvII, 7µm/h.

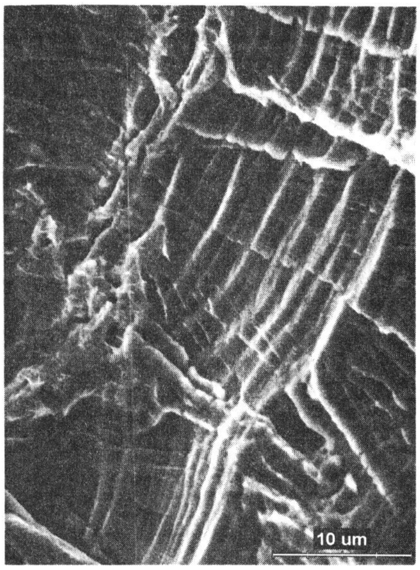

Fig.8: The crack surface in EnvII, 49µm/h.

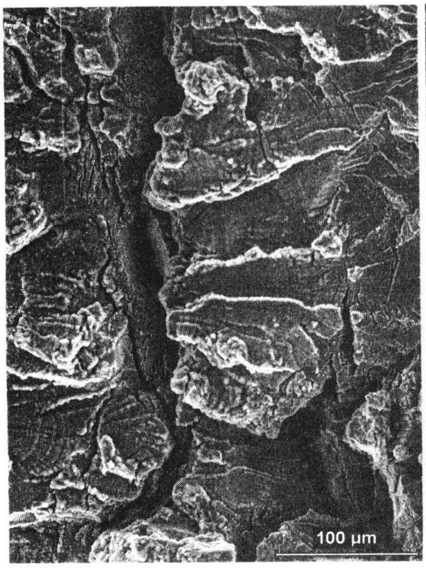

Fig.9: EAC- pre-fatigue interface, EnvIII.

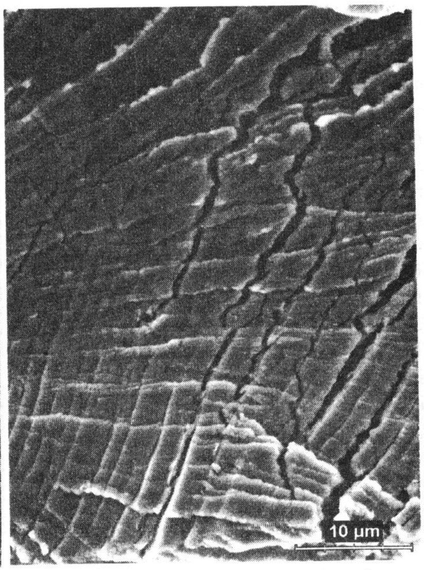

Fig.10: Detail of Fig9., EnvIII, 23µm/h.